

Kinetics of Photodegradation and Nanoparticle Surface Accumulation of a Nanosilica/Epoxy Coating Exposed to UV Light

Lipiin Sung,¹ Justin M. Gorham,² Deborah Stanley,¹ Hsiang-Chun Hsueh,¹ Savelas Rabb,² Lee L. Yu,² Chun-Chieh Tien¹
and Tinh Nguyen¹

¹*Engineering Laboratory*

²*Material Measurement Laboratory*

National Institute of Standards and Technology, Gaithersburg, MD, USA

Abstract

Temperature effect on the kinetics of photodegradation, surface accumulation of nanoparticles, and nanoparticle release in an epoxy nanocoating exposed to ultraviolet light (UV) was investigated. A model epoxy coating containing 5 % untreated nanosilica was selected. Exposed film specimens were removed at specified UV dose intervals for measurements of chemical degradation of the epoxy component, nanosilica accumulation on specimen surface, and nanosilica release as a function of UV dose for four temperatures. The chemical degradation was measured using Fourier transform infrared spectroscopy (FTIR), X-ray photoelectron spectroscopy (XPS), and UV-visible spectroscopy (UV-Vis). Atomic force microscopy (AFM) was employed to determine the kinetics of nanosilica accumulation on the nanocoating surface during UV exposure. The temperature dependence behaviors of kinetic parameters obtained by various measurement techniques will be used to better understand the degradation mechanism and surface accumulation of nanoparticles in exterior nanocoatings.

INTRODUCTION

Polymeric materials containing nanofillers (polymer nanocomposites) have attracted growing interest due to their outstanding properties as well as their unique applications[1-5]. Polymer nanocoatings, a subclass of nanocomposites, are increasingly used outdoors such as on building structures, airplanes, and automobiles, because of their excellent mechanical, gas barrier, self-cleaning, and UV resistance properties.

Studies have long indicated that most common polymers undergo significant degradation during exposures to outdoor environments [6-8]. A serious consequence of the matrix degradation for nanocoatings is that the nanofillers embedded in the polymer matrices could be released via the effect of rain, snow, condensed water, and wind. Such nanoparticle release during nanocoating life cycle is a concern, because engineered nanofillers have been shown to be hazardous to the environment and human health [9-11].

Taking advantage of the highly uniform and high intensity UV radiation from the SPHERE device (Simulated Photodegradation via High Energy Radiant Exposure) [12], the National Institute of Standards and Technology (NIST) has investigated the degradation rate, nanomaterial surface accumulation, and nanomaterial release for a model epoxy (without UV stabilizers) containing silica nanoparticles [13-16]. In a previous study on an amine-cured epoxy nanocoating exposed to UV radiation at 60 °C/ \approx 0 % relative humidity (RH) exposure condition, we have found that the epoxy matrix in the nanocoating underwent rapid photodegradation during exposure to 295 nm to 400 nm UV, exposing nanosilica on the surface and subsequently releasing it from the nanocoating [13].

Although nanosilica accumulated on the surface and subsequent release from the nanocoatings was observed and measured [13], the role of temperature on the photodegradation rate, surface accumulation and release of nanoparticles has not been investigated. Temperature is an important factor in the degradation process of polymers. In this study, we examined how temperature affects the both the photodegradation of polymer matrix and surface accumulation (and possible release) of nanosilica during UV exposures of an epoxy nanocoating. The resulting knowledge of temperature dependence behaviors on kinetic parameters obtained by different measurements will be useful for understanding the degradation mechanism and predicting the long term release of nanoparticles in exterior nanocoatings.

EXPERIMENTAL PROCEDURES

Materials and Preparation of Nanocoating

Unless stated, the silica nanoparticles (i.e., nanosilica) were an untreated material in powder form, having a normal diameter of 15 nm and a purity greater than 99.5 % (provided by manufacturer). The epoxy coating was a model stoichiometric mixture of a diglycidyl ether of bisphenol A (DGEBA) epoxy resin having an equivalent mass of 189 (grams of resin containing one gram equivalent of epoxide) and a tri-polyetheramine curing agent. There were no UV stabilizers added to the amine-cured epoxy coating. It should be noted that, due to steric hindrance and restricted transport during the late curing stages, some residual unreacted epoxide and amino groups are expected to be present in the coating films after curing. The presence of these functional groups and impurities (e.g., residual catalysts, processing aids, etc.) may have an influence on the photodegradation of an amine-cured epoxy coating. The solvent used for nanoparticle dispersion and coating processing was reagent grade toluene (purity > 99.5 %). The chemical structures of the components and the cured epoxy coating are given elsewhere [16]. Free-standing films having a thickness between 125 μ m and 150 μ m of the amine-cured epoxy containing 5 % mass fraction of nanosilica were prepared following the procedure described in Ref. [15]. All films were cured at ambient conditions (24 °C and 50 % RH) for 1 d, followed by post-curing for 45 min at 110 °C in an air circulating oven. The quality of all epoxy/nanosilica coating (epoxy nanocoating) films was assessed by visual inspection for evidence of air bubbles or defects (cracks). Specimens were only selected from defect-free regions.

UV Exposure

Specimens of epoxy nanocoating were exposed to < 1 % RH at four different temperatures, 30 °C, 40 °C, 50 °C, and 60 °C in the NIST SPHERE UV chamber [12]. The very dry condition was used to

minimize any effect of water on the photodegradation of epoxy. The NIST SPHERE UV chamber produces a highly uniform UV flux of approximately 140 W/m^2 in the wavelength range of 295 nm to 400 nm. Specimens for characterizing surface morphology had a dimension of 10 mm x 10 mm and those for tracking chemical changes had a diameter of 19 mm. Specimens were removed after specified accumulated UV doses (i.e., at specified time intervals) for various characterizations. UV dose, in MJ/m^2 , is defined here as the total accumulated energy resulting from repeated UV radiation exposures at a particular time period per unit irradiated surface. Because the SPHERE was operated without interruption during this experiment, its UV dose is linearly proportional to exposure time.

Characterization of Nanocoating Degradation and Surface Morphological changes

The chemical degradation of both neat epoxy and nanocoating was measured using molecular spectroscopy via attenuated total reflection Fourier transform infrared spectroscopy (ATR-FTIR), X-ray photoelectron spectroscopy (XPS), and UV-visible spectroscopy (UV-Vis). ATR-FTIR spectra were recorded at a resolution of 4 cm^{-1} using dry air as a purge gas and a spectrometer (Nexus 670, Thermo Nicolet) equipped with a liquid nitrogen-cooled mercury cadmium telluride (MCT) detector. A ZnSe prism and 45° incident angle were used for the ATR-FTIR measurement. All spectra were the average of 128 scans. The peak height was used to represent the infrared intensity, which is expressed in absorbance, A. All FTIR results were the average of four specimens. UV-Visible spectra were recorded using an HP 8452A spectrometer fitted with an autosampler. Spectra were collected for wavelengths from 190 nm to 1100 nm with an integration time of 0.5 s.

XPS was used for elemental and chemical state analysis of the nanocoatings. Analyses were carried out using an Axis Ultra DLD spectrophotometer (Kratos Analytical) equipped with a monochromated Al K α X-ray source (1486.6 eV). The photoelectrons were collected along the surface normal at a pass energy 40 eV and a step size of 0.1 eV/step for the C(1s), Si(2p), O(1s) and N(1s) regions. All XPS spectra were fit with a Shirley baseline and adjusted with the appropriate elemental sensitivity factors to obtain information on percent composition.

Surface morphological changes of nanocoating were followed by tapping mode atomic force microscopy (AFM) at ambient conditions (24 °C, 50 % RH) using a Dimension 3100 system (Veeco Metrology) and silicon probes (TESP 70, Veeco Metrology). Both topographic (height) and phase images were obtained simultaneously using a resonance frequency of approximately 300 kHz for the probe oscillation and a free-oscillation amplitude of $62 \text{ nm} \pm 2 \text{ nm}$.

RESULTS

Surface Morphological Changes

Figure 1 displays AFM height and phase images of unexposed and UV-exposed epoxy nanocoating surface at, as an example, 40 °C. Contrast in the height images of Figure 1a is due to the surface topography, with little evidence of nanoscale particles being present on the surface, which is also confirmed in the featureless phase image (Figure 1a, right). As the UV dose increased, the surface roughness increased and nanoparticles or clusters of nanoparticles appeared on the surface, as shown in both the height and phase images of Figure 1b. Brightness of the particles in the height image indicates that they were above the surface. The phase image also shows a strong contrast between the nanoparticles and the matrix, which is typically observed for mixtures of a high modulus inorganic material and a low modulus polymeric material.

Figure 2 shows the surface morphological changes of the nanocoating exposed to different UV doses in four temperatures (30 °C, 40 °C, 50 °C, and 60 °C). All four temperatures showed similar effects. The number of particles on the surface increased with increasing UV dose, and the size of the particle clusters and the number of connected clusters also increased with UV dose. After 400 MJ/m^2 dose, a layer of compact particles almost covered the entire surface for all four temperatures. Similar results were observed in NIST previous studies for a silane-treated nanosilica in a similar epoxy system [8, 16].

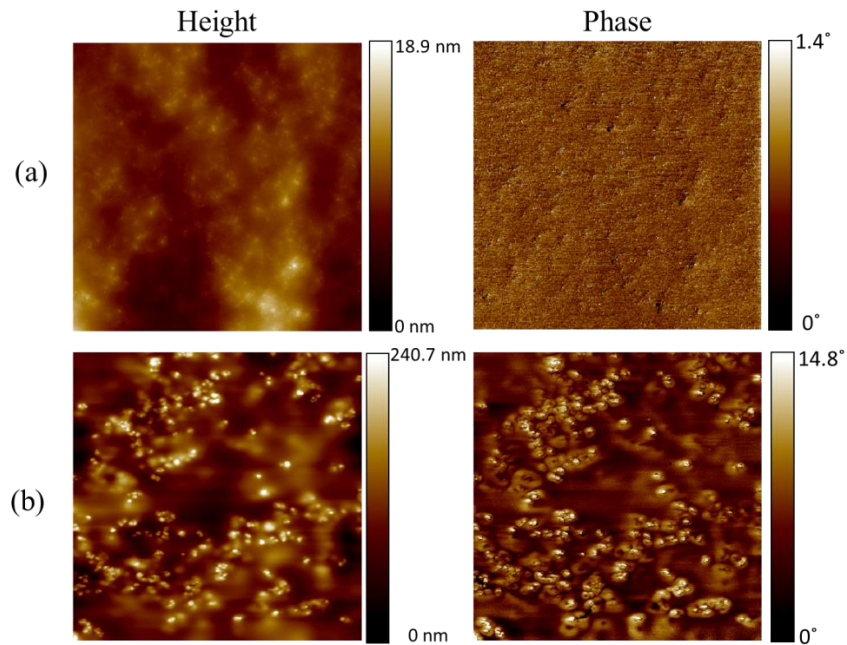


Figure 1 AFM height images (left column) and phase images (right column) of nanocoating (a) unexposed and (b) exposed for 30 MJ/m² UV dose and at 40 °C. Scan size is 20 μm × 20 μm. The scale bars represent the height and phase range of each image.

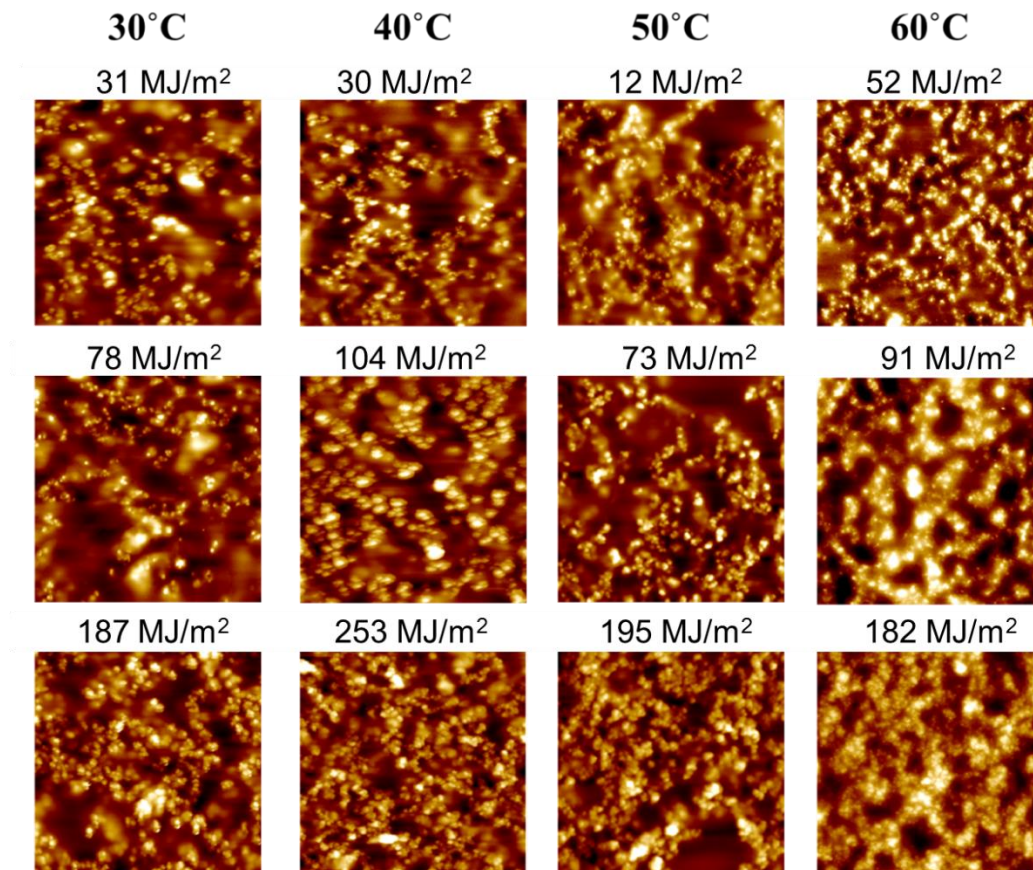


Figure 2: AFM height images of epoxy nanocoating as a function of UV doses for four different temperatures; scan size: 20 μm × 20 μm. The height range of the images are roughly from 0 nm to 1.5 μm.

To follow the accumulation of nanosilica on the nanocoating surface during UV exposure, an AFM software image analysis was conducted. Figure 3 displays the surface coverage (in %) of revealed particles (assuming as nanosilica clusters) as a function of UV dose. It shows that the accumulation of nanosilica on the UV-exposed nanocoating increased rapidly between 0 MJ/m² and 300 MJ/m² dose but slowed down substantially thereafter. The shape of nanosilica coverage vs. UV dose curve is similar to the chemical changes such as oxidation measured by FTIR with UV dose [13], suggesting that the accumulation of nanosilica on the nanocoating surface with UV exposure is closely related to photodegradation of the epoxy matrix. That is, as the epoxy layer on the nanocoating surface was degraded by UV radiation, silica nanoparticles that were embedded in the matrix were increasingly exposed on the surface. Figure 3 shows that a higher exposure temperature resulted in a higher amount of surface accumulation of nanosilica for dose less than 600 MJ/m². For example, at an exposure dose of 400 MJ/m², the surface coverages were approximately 45 %, 50 %, 56 %, and 60 % for 30 °C, 40 °C, 50 °C, and 60 °C, respectively. However, at doses of 700 MJ/m² or greater, there was essentially no difference in surface coverage between 50 °C and 60 °C.

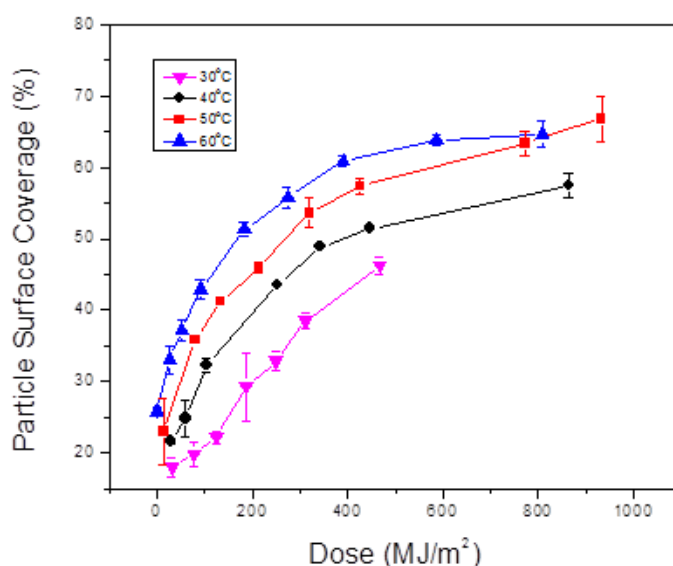


Figure 3. Nanosilica coverage on epoxy nanocoating surface as a function of UV dose at four different temperatures as indicated in the legend. Each data point is the average of three measurements (20 $\mu\text{m} \times 20 \mu\text{m}$ scan area). The error bars represent one standard deviation.

Chemical Degradation

Figure 4 displays the chemical degradation of an amine-cured epoxy nanocoating exposed to UV radiation at four different temperatures measured by FTIR-ATR technique. The bands at 1245 cm⁻¹ and 1724 cm⁻¹, representing chain scission and oxidation of the epoxy, respectively, and at 1060 cm⁻¹, attributed to both epoxy C-O and Si-O bonds, were used to follow various degradation processes and surface accumulation of silica nanoparticles of nanocoating during UV exposure. Intensity changes of these bands after normalization to 1380 cm⁻¹ with UV dose are displayed in Figure 4. The error bars in Figure 4 show small standard deviations (except at high UV dose), indicating a good reproducibility between specimens. Detailed description of FTIR data analyses was reported in Reference [13]. As shown in Figures 4a and 4b, the intensity of the bands at 1245 cm⁻¹ and 1724 cm⁻¹ changed rapidly at shorter/lower exposure time/dose (< 200 MJ/m²), but reached a plateau value for dose > 400 MJ/m². The 60 °C data shows a highest degradation rate (a fewer data points than other temperature because of rapid degradation) among the four temperatures. The intensity of the band at 1060 cm⁻¹ (Figure 4c) increased with increasing UV dose, suggesting that silica has gradually accumulated on the specimen surface. However, there was no clear trend in the temperature effect on this combined C-O and Si-O band. This is probably a result of two oppositely competing processes taking place on

the nanocomposite surface during UV irradiation: loss of epoxy material (C-O loss) and increase of silica nanoparticles on the surface (Si-O increase).

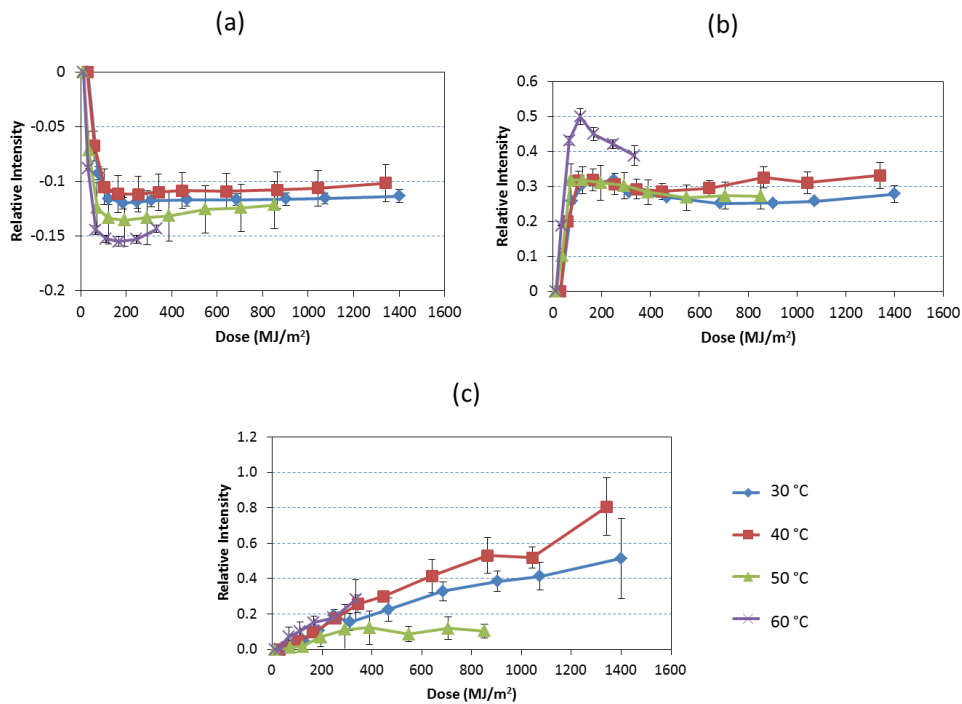


Figure 4. ATR-FTIR relative intensity changes with UV dose at four temperatures for bands at: a) 1245 cm^{-1} , b) 1724 cm^{-1} , and c) 1060 cm^{-1} . The intensities have been normalized to that of the band at 1380 cm^{-1} . The results are average of 6 specimens, and error bars represent one standard deviation.

In addition to FTIR data, UV-Vis measurements were also carried out on thinner nanocoating specimens (a 7 μm film on a CaF_2 substrate) to obtain the chemical degradation rate at various exposure temperatures. Figure 5 displays the chemical changes via UV-Vis absorbance at wavelength (λ) = 354 nm for both neat epoxy and nanocoatings at four different exposure temperatures. In both materials, the absorbance increased as UV dose increased, and higher temperature had a higher rate of increase.

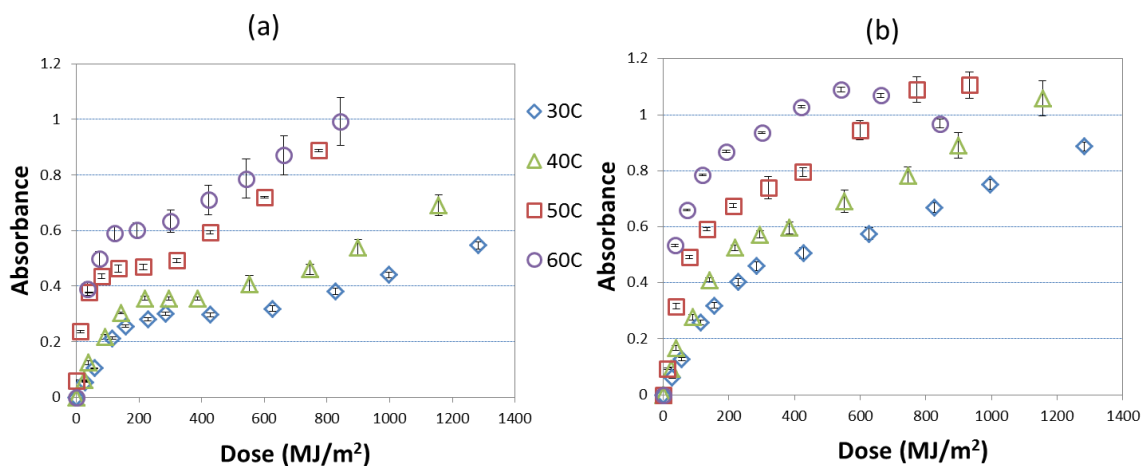


Figure 5. UV-visible intensity at $\lambda = 354 \text{ nm}$ as a function of UV dose for (a) neat epoxy and (b) nanocoating for four different temperatures. The results are average of 4 specimens, and error bars represent one standard deviation. All absorbance values presented here are subtraction from values at exposure time = 0.

To detect the chemical composition on the nanocoating surface, XPS measurements were performed on the same samples after AFM measurements. Figure 6 displays the XPS-based carbon (C), oxygen (O), nitrogen (N), and silicon atomic (Si) percentages on the epoxy/nanosilica coating surface vs. exposure time. The loss of the epoxy matrix and an increase of the silica material near the nanocoating surface as a function of exposure time (proportional to dose) observed by ATR-FTIR in Figure 4a and 4c are consistent with the XPS results displayed in Figure 6. As the UV dose increased from 0 MJ/m² to 770 MJ/m² (\approx 60 d) at 60 °C exposure condition, the percent surface concentrations of carbon decreased from 77.4 % \pm 1.4 % to 50.2 % \pm 1.7 %, while those of silicon started at 3.4 % \pm 0.8 %, dropped after a small dose of 54 MJ/m² to 0.9 % \pm 0.1 % followed by a steady rise to a final value of 6.5 % \pm 0.4 %, and nitrogen increased from 1.4 % \pm 0.2 % to 8.1 % \pm 0.2 %. The increase of nitrogen with UV dose observed in Figure 6 for nanosilica composite may be explained as due to the adsorption of the base amine curing agent on the acidic nanosilica surface during mixing and film formation. In this case, the adsorbed amine would form an interfacial layer between the silica nanoparticles and the epoxy polymer. Discussion on the formation of this interfacial layer is described in Ref [13].

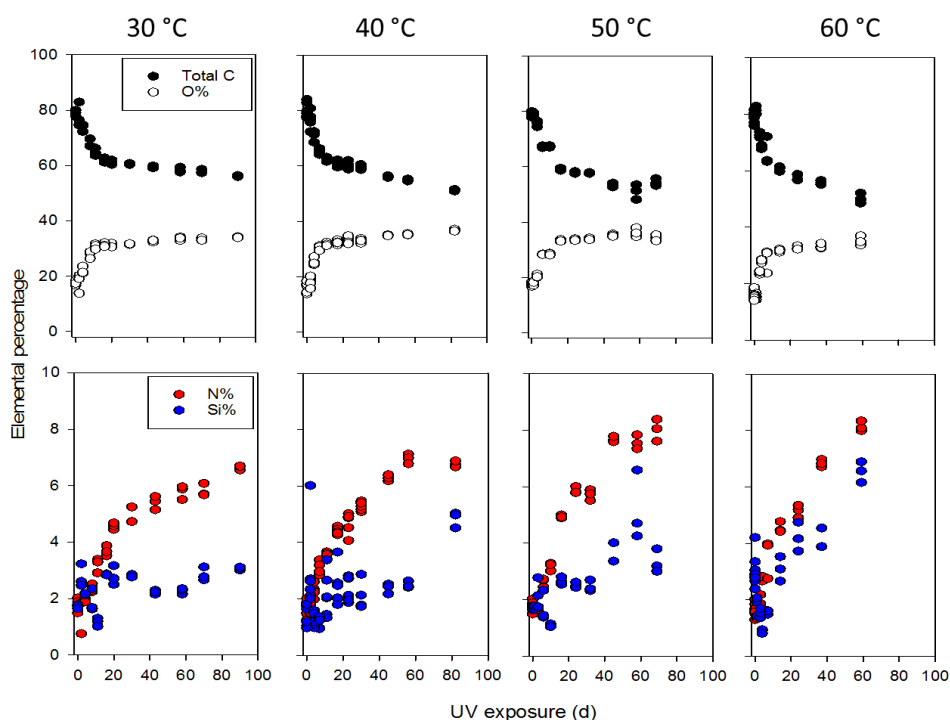


Figure 6. XPS-based carbon, nitrogen, and silicon atomic percentages on the epoxy/nanosilica coatings surface vs. UV exposure time (d). At same exposure times, more than two locations were measured as shown in the graphs.

To get a better comparison visually, the increase of Si element percentage at different temperatures was plotted vs. UV dose for four different temperatures; the results are displayed in Figure 7. For doses less than 200 MJ/m², all data scattered around 2 % with large error bars for all temperatures. Except for 50 °C exposure condition, the data do not follow a steady increase with temperature, and the last data point drop unexpectedly. In general, a higher exposure temperature resulted in a higher amount of Si element percentage for doses > 200 MJ/m². However, the Si(2p) percentages increased with UV dose at a rate that increased with temperature. Extrapolated based on a linear fit of measurements (dose > 0 MJ/m²) at each temperature (not shown), the Si percentage that is at the surface for 600 MJ/m² is 2.5 % \pm 0.1 %, 2.8 % \pm 0.2 %, 3.6 % \pm 0.3 %, and 5.4 % \pm 0.4 % for 30 °C, 40 °C, 50 °C, and 60 °C, respectively. This result is in agreement with nanosilica surface accumulation data obtained by AFM measurements shown in Figure 3.

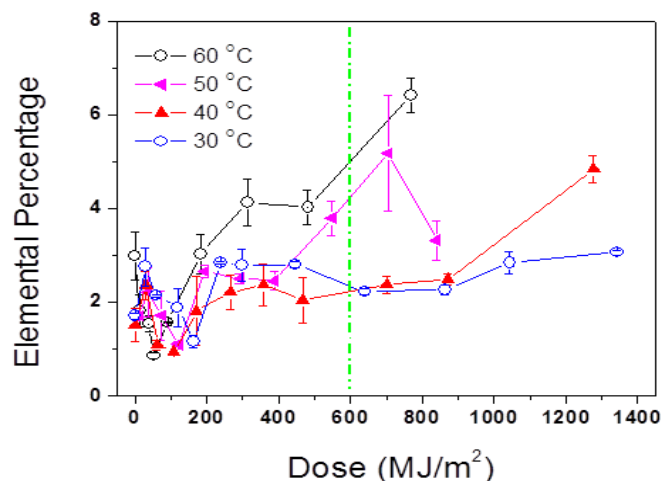


Figure 7. XPS-based silicon (Si) % elemental percentage on the epoxy/nanosilica coatings surface vs. UV irradiation dose at four different temperatures. Each data point consists of two or more specimens and the error bars represent one standard deviation. The dashed line indicates the dose at 600 MJ/m².

CONCLUDING REMARKS

The effects of temperature on both the photodegradation of epoxy matrix and surface accumulation of nanosilica during UV exposures of an epoxy coating containing 5 mass % nanosilica were investigated through a suite of techniques, such as FTIR, XPS, UV-Vis, and AFM. All results indicated that the higher temperature, the higher photodegradation and surface nanosilica accumulation rate. The chemical degradation rate of the matrix (via FTIR data in Figures 4a & 4b, UV-Vis data in Figure 5), and accumulation rate for Si on the surface (via AFM: Figure 3 and via XPS data in Figure 6) followed the right temperature order, i.e., 60 °C > 50 °C > 40 °C > 30 °C. Further data analyses are on going to obtain degradation kinetic parameters for nanocoatings exposed to various UV/temperature/humidity conditions. Kinetics data of polymer coatings containing nanoparticles under different UV environments is essential for better understanding the degradation mechanism and predicting the release of nanoparticles from exterior nanocoatings.

DISCLAIMER

Certain commercial product or equipment is described in this paper in order to specify adequately the experimental procedure. In no case does such identification imply recommendation or endorsement by the National Institute of Standards and Technology, nor does it imply that it is necessarily the best available for the purpose.

REFERENCE

- [1] Podsiadlo, P, Kaushik, AK, Arruda, EM, Waas, AM, Shim, BS, Xu, J, et al., "Ultrastrong and stiff layered polymer nanocomposites," *Science*, vol. 318, pp. 80-3, Oct 5 2007.
- [2] Crosby, AJ, and Lee, YJ "Polymer Nanocomposites: The "Nano" Effect on Mechanical Properties," *Polymer Reviews*, vol. 47, pp. 217-229, 2007.
- [3] Croce, F, Appetecchi, G, Persi, L, and Scrosati, B, "Nanocomposite polymer electrolytes for lithium batteries," *Nature*, vol. 394, pp. 456-458, 1998.
- [4] Ramanathan, T, Abdala, AA, Stankovich, S, Dikin, DA, Herrera-Alonso, M, Piner, RD, et al., "Functionalized graphene sheets for polymer nanocomposites," *Nat Nanotechnol*, vol. 3, pp. 327-31, Jun 2008.

- [5] Shah, MSA, Nag, M, Kalagara, T, Singh,S, and Manorama, S V, "Silver on PEG-PU-TiO₂ polymer nanocomposite films: An excellent system for antibacterial applications," *Chemistry of Materials*, vol. 20, pp. 2455-2460, 2008.
- [6] Sung, LP, Jasmin, J, Gu, XH, Nguyen,T, and Martin, JW, "Use of laser scanning confocal microscopy for characterizing changes in film thickness and local surface morphology of UV-exposed polymer coatings," *J. Coat. Technol. Res.*, vol. 1, pp. 267-276, 2004.
- [7] Nguyen, T, Martin, J, Byrd, E, and Embree, N,"Relating laboratory and outdoor exposure of coatingsIII. Effect of relative humidity on moisture-enhanced photolysis of acrylic-melamine coatings," *Polymer Degradation and Stability*, vol. 77, pp. 1-16, 2002.
- [8] Nguyen,T, Pellegrin,B, Bernard, C, Gu, X, Gorham, JM, Stutzman, P, *et al.*, "Fate of nanoparticles during life cycle of polymer nanocomposites," *Journal of Physics: Conference Series*, vol. 304, p. 012060, 2011.
- [9] Jin, Y, Kannan, S, Wu, M, and Zhao, JX, "Toxicity of luminescent silica nanoparticles to living cells," *Chem Res Toxicol*, vol. 20, pp. 1126-33, Aug 2007.
- [10] Lin, W, Huang, JW, Zhou, XD, and Ma, Y, "In vitro toxicity of silica nanoparticles in human lung cancer cells," *Toxicol Appl Pharmacol*, vol. 217, pp. 252-9, Dec 15 2006.
- [11] Lin, YS, and Haynes, CL, "Impacts of mesoporous silica nanoparticle size, pore ordering, and pore integrity on hemolytic activity," *J Am Chem Soc*, vol. 132, pp. 4834-42, Apr 7, 2010.
- [12] Chin, J, Byrd, E, Embree,E, *et al.*, "Accelerated UV weathering device based on integrating sphere technology," *Rev. Sci. Instrum.* Vol. 75, pp. 4951-4959, 2004.
- [13] Sung, L, Stanley, D, Gorham, JM, Rabb, SA, Gu, X, Yu, LL, Nguyen, T, "A quantitative study of nanoparticle release from nanocoatings exposed to UV radiation," *J. Coat. Technol. Res.*, Vol. 12, no1, pp. 121-135, 2015.
- [14] Nguyen, T, Pellegrin, B, Bernard, C, Gu, X, Gorham, JM, Stutzman, P, Stanley, D, Shapiro, A, Byrd, E, Hettenhouser, R, Chin, J, "Fate of nanoparticles during life cycle of polymer nanocomposites," *J. Phys.: Conf. Ser.*, 304 012060, 2011.
- [15] Gorham, JM, Nguyen, T, Bernard, C, Stanley, D, Holbrook, RD, "Photo-induced surface transformations of silica nanocomposites," *Surf. Interface Anal.*, Vol. 44, pp. 1572-158, 2012.
- [16] Nguyen, T, Pellegrin, B, Bernard, C, Rabb, S, Stutzman, P, Gorham, JM, Gu, X, Yu, LL, Chin, J, "Characterization of surface accumulation and release of nanosilica during irradiation of polymer nanocomposites by ultraviolet light." *J. Nanosci. Nanotechnol.*, Vol. 12, pp. 6202-6215, 2012.
- [17] Stanley, D, Huang, SR, Cheng, YL, Rabb, S, Gorham, JM, Krommenhoek, PJ, Yu, LL, Nguyen, T and Sung, L, "Investigating the Process of Surface Degradation and Nanoparticle Release of a Commercial Nanosilica / Polyurethane Coating Under UV Exposure," Accepted for *publication*, *J. Coat. Technol. Res.*, Dec., 2015.